A Systematic Way to Extend the Debye-Hückel Theory Beyond Dilute Electrolyte Solutions

Tiejun Xiao[†] and Xueyu Song[*,‡]

†*Guizhou Provincial Key Laboratory of Computational Nano-Material Science, Guizhou Synergetic Innovation Center of Scientific Big Data for Advanced Manufacturing Technology, Guizhou Education University, Guiyang 550018 People's Republic of China*

‡*Department of Chemistry and Ames Laboratory, Iowa State University, Ames, IA 50011*

E-mail: xsong@iastate.edu

Abstract

An extended Debye-Hückel theory with fourth order gradient term is developed for electrolyte solutions, namely the electric potential $\varphi(\mathbf{r})$ of the bulk electrolyte solution can be described by $\nabla^2\varphi(r) = \kappa^2\varphi(r) + L_Q^2\nabla^4\varphi(r)$, where the parameters κ and L_Q are chosen to reproduce the first two roots of the dielectric response function of the bulk solution. Three boundary conditions for solving the electric potential problem are proposed based upon the continuity conditions of involving functions at the dielectric boundary, with which a boundary element method for the electric potential of a solute with a general geometrical shape and charge distribution is derived. Solutions for the electric potential of a spherical ion and a diatomic molecule are found and used to calculate their electrostatic solvation energies. The validity of the theory is successfully demonstrated when applied to binary as well as multi-component primitive models of electrolyte solutions.

1 Introduction

Mean field theories for electrolyte solutions or ionic fluids in general have been widely used in solvation and crystallization processes,[1–4] surface tension calculations[5–8] and electron transfer processes.[9–12] A major challenge in the theory of electrolyte solutions is to answer how an electrolyte solution is polarized by a charged solute. Nowadays it is well known that an ion is perfectly screened by the electrolyte solution as indicated by the Debye-Hückel (DH) theory.[13] The DH response equation for the electric potential $\varphi(\mathbf{r})$, which is also known as linearized Poisson-Boltzmann equation, reads $\nabla^2\varphi(\mathbf{r}) = \kappa_D^2\varphi(\mathbf{r})$, where κ_D is the inverse Debye length and ∇^2 the Laplacian. According to the DH theory, the electric potential of a point charge satisfies the Yukawa form as $\varphi(r) = \frac{q}{\epsilon_s}\frac{e^{-\kappa_D r}}{r}$. One important feature of the DH theory is the existence of a boundary element method for a solute with general geometry and charge distribution, which can reduce the original three dimensional electric potential problem to a two dimensional electric potential problem on the molecular surface.[14–16] Such

a property renders the DH theory especially useful for studying the electrostatic interaction between complex biomolecules in an electrolyte solution.[17–20] On the other hand, the linearization of the Poisson-Boltzmann equation relies on the weak coupling assumption, hence the application of DH theory is limited to dilute electrolyte solutions.[20,21]

There are various efforts to understand the screening effect of electrolyte solutions and why the DH theory fails for concentrated electrolyte solutions. According to the rigorous analysis from statistical mechanics, the electric potential of an ion undergoes a transition from simple exponential decay to oscillatory decay as the electrostatic coupling of the solution varies from weak to strong.[22–25] Such an effect is known to originate from the competition between the local packing effect and the long ranged Coulomb interaction.[26–28] Kjellander and coworkers developed a dressed ion theory based on a rigorous charge renormalization process of the Poisson-Boltzmann equation, where the electric potential can be casted into a DH-like form $\nabla^2\varphi(\mathbf{r}) = \int B(|\mathbf{r}-\mathbf{r}'|)\varphi(\mathbf{r}')d\mathbf{r}' + \frac{4\pi}{\epsilon_0}\rho^0(\mathbf{r})$, where $B(r)$ is a local response function of the bulk solution and $\rho^0(\mathbf{r})$ is an effective charge density of the solute.[29–31] Such a result can also be obtained from the dispersion relations of Maxwell equations[32,33] with a microscopic model of electrolyte solutions. In the dilute limit, the dressed ion theory reduces to the DH theory as $\rho^0(\mathbf{r}) = q\delta(\mathbf{r})$ and $B(r) = \kappa^2\delta(r)$. According to the asymptotic analysis, the dressed ion theory leads to multi-Yukawa electric potentials for concentrated electrolyte solutions, namely, $\varphi(r) \sim \sum_l \frac{q_l^* e^{-k_l r}}{\epsilon_l r}$, where q_l^* is a renormalized charge, ϵ_l is an effective dielectric constant. The decay parameters $\{k_l\}$ are determined by the roots of the bulk dielectric function and become complex numbers in the strong coupling regime, hence the oscillatory decaying potentials are naturally recovered. In practical applications, the decay parameters of the electric potential in electrolyte solutions can be derived from the theory of electrolyte solutions[29,34–37] or measured from experiments,[38,39] and hence can be used to evaluate thermodynamic properties.

As a single Yukawa potential is the solution of the DH response equation, a multi-Yukawa potential from rigorous analysis motivates us to build a multi-DH response theory for concen-

trated electrolyte solutions. In our previous work,[33] the molecular DH theory is developed for various models of electrolyte solutions, where the electric potential $\varphi(r)$ of an ion splits into a linear combination of individual modes, i.e., $\varphi(r) = \sum_l B_l \varphi_l(r)$ and $\nabla^2 \varphi_l(r) = k_l^2 \varphi_l(r)$ in bulk electrolyte solutions. The linear coefficients $\{B_l\}$ can be determined in a self-consistent way to reproduce the dielectric response function of the pure solvent. Such a prescription has been applied successfully to various ionic fluids.[40–44] As the molecular DH theory is mainly developed for spherical ions and it remains an open question to deal with solutes beyond spherical geometry.

In this paper, we developed an extended Debye-Hückel(EDH) theory which not only leads to multi-Yukawa potential for spherical ions but can also be easily applied to solutes with arbitrary geometry and charge distribution using boundary element method. Specifically, a fourth order gradient term $L_Q^2 \nabla^4 \varphi(r)$ is introduced to the dielectric response equation, which will have two Debye screening lengths as a first step to a general solution with more Debye screening lengths in a straight-forward manner. In order to uniquely determine the electric potential, three boundary conditions are required and the corresponding boundary element method is developed. Our theory leads to analytical electric potentials as well as electrostatic solvation energies for a spherical ion and a diatomic molecule solute, and is tested successfully against the mean spherical approximation (MSA) theory, the hyper-netted chain (HNC) theory and molecular dynamics(MD) simulations of electrolyte solutions.

It should be emphasized that the goal of this work is not to develop a self-consistent theory of electrolyte solutions, a worthwhile endeavor itself, but rather to extend the applicability of the widely used boundary element method of electrostatics in biophysics to moderately coupled electrolyte solutions.

This paper is organized as following: in section 2 the EDH theory of electrolyte solutions is formulated. The excess thermodynamic properties for electrolyte solutions are also discussed. In section 3 the EDH theory is applied to electrolyte solutions where direct comparisons with MSA theory, HNC theory and MD simulations demonstrate the accuracy of our theory. Some

concluding remarks are given in section 4.

2 Theory

2.1 Model description of the primitive model of electrolyte solutions

The restricted primitive model of an electrolyte solution is taken as a mixture of ions with additive hard spheres where a point charge at the center immersed in a dielectric continuum. Cations and anions of the solvent have the same diameter σ_s and the same absolute charge q_s. In the field of physical chemistry, the concept of solvent is widely used to represent the polar species of the solutions. As the polar species are not considered explicitly in the restricted primitive model, hereafter the electrolyte solution itself is taken as the solvent and a tagged molecule is taken as a solute. Denote k_B as the Boltzmann constant, T as the temperature, n_s as the total particle number density and ϵ_s as the dielectric constant of the dielectric continuum, the reduced inverse temperature is $\beta = \frac{1}{k_B T}$, the Debye parameter is $\kappa_D = \sqrt{\frac{4\pi\beta n_s q_s^2}{\epsilon_s}}$.

A molecular solute with N sites is described by an interaction site model, where a site j is a sphere with diameter σ_j and carries a point charge q_j at point $\mathbf{r}_j$. Ω_1 is the volume of the solute, Ω_2 is the volume outside the solute, and Σ is the molecular surface.

2.2 An extended Debye-Hückel(EDH) dielectric response model and boundary conditions

In general, the dielectric function of a solvent can have many Debye screening lengths,[29,33] but as a first step to develop a full theory of their dielectric response, we concentrate on the two Debye screening lengths case, which is equivalent to a mixture of ions with quadrupole response.[45] Let $\phi(\mathbf{r})$ be the electric potential in a solute, where $\mathbf{r} \in \Omega_1$; $\psi(\mathbf{r})$ be the electric

potential outside the solute, where $\mathbf{r} \in \Omega_2$, then we have

$$\nabla^2\phi(\mathbf{r}) = -\frac{4\pi}{\epsilon_s}\rho^b(\mathbf{r}), \qquad \mathbf{r} \in \Omega_1 \tag{1}$$

$$\nabla^2\psi(\mathbf{r}) = \kappa^2\psi(\mathbf{r}) + L_Q^2\nabla^4\psi(\mathbf{r}), \qquad \mathbf{r} \in \Omega_2 \tag{2}$$

where $\rho^b(\mathbf{r}) = \sum_{j=1}^{N} q_j\delta^{(3)}(\mathbf{r} - \mathbf{r}_j)$ is the bare charge density of the solute. κ is an effective Debye parameter and L_Q is a length scale related to the quadruple effect. In the limit $L_Q = 0$, the dielectric response equation reduces to the conventional DH equation.

In order to determine the electric potential problem with fourth order gradient term, three boundary conditions are needed. However, as there is no unique choice for these boundary conditions different researchers used different recipes[45–49] with various physical arguments. On the other hand, these boundary conditions can be stated mathematically using the continuity of functions across the boundary as pointed out in Stakgold's book,[50] which reflects physical conservation laws. In general, there are four possible boundary conditions, which are related to the continuity of $\psi(\mathbf{r})$, $\frac{\partial\psi(\mathbf{r})}{\partial n}$, $\nabla^2\psi(\mathbf{r})$, and $\frac{\partial\nabla^2\psi(\mathbf{r})}{\partial n}$, where $\mathbf{n}$ is the outward unit normal to Σ at $\mathbf{r}$. However, only three boundary conditions are necessary to determine the electric potential problem due to the lack of fourth order gradient term inside the solute. In our formulation, the continuity of $\psi(\mathbf{r})$, $\frac{\partial\psi(\mathbf{r})}{\partial n}$ and $\frac{\partial\nabla^2\psi(\mathbf{r})}{\partial n}$ are used as boundary conditions. Let $\mathbf{r}_0$ be a point on the molecular surface Σ, then the boundary conditions read

$$\lim_{\mathbf{r}\to\mathbf{r}_0}\psi(\mathbf{r}) = \lim_{\mathbf{r}\to\mathbf{r}_0}\phi(\mathbf{r}), \tag{3}$$

$$\lim_{\mathbf{r}\to\mathbf{r}_0}\frac{\partial\psi(\mathbf{r})}{\partial n} = \lim_{\mathbf{r}\to\mathbf{r}_0}\frac{\partial\phi(\mathbf{r})}{\partial n}, \tag{4}$$

$$\lim_{\mathbf{r}\to\mathbf{r}_0}\frac{\partial\nabla^2\psi(\mathbf{r})}{\partial n} = \lim_{\mathbf{r}\to\mathbf{r}_0}\frac{\partial\nabla^2\phi(\mathbf{r})}{\partial n}. \tag{5}$$

The first two boundary conditions are the same as the ones widely used in the DH theory. It is noted that Eq.(4) is valid for the interaction site model where no surface charge density is present. If there is a surface charge $\sigma(\mathbf{r}_0)$ on the molecular surface, then the Eq.(4) should

be modified as $\lim_{\mathbf{r}\to\mathbf{r}_0}\frac{\partial\psi(\mathbf{r})}{\partial n}=\lim_{\mathbf{r}\to\mathbf{r}_0}\frac{\partial\phi(\mathbf{r})}{\partial n}-\frac{4\pi\sigma(\mathbf{r}_0)}{\epsilon_s}$. One may note that it is also possible to replace Eq.(5) by the continuity of $\nabla^2\varphi(\mathbf{r})$ as the third boundary conditions. Note that $\nabla^2\psi(\mathbf{r})$ is linearly related to the induced charge density which is known to be discontinuous on the molecular surface due to the hard sphere interactions. Our numerical results also show that the electrostatic energies for spherical ions from this route is not accurate. To this end, the continuity of $\nabla^2\varphi(\mathbf{r})$ is not suggested as a good choice for the third boundary condition.

2.3 Integral equations for the boundary element method

In this part we use Juffer *et al*'s prescription[14] to formulate a boundary element method for systems described by Eqs.(1) and (2). The main idea of boundary element method is to reduce the original three-dimensional electric potential problem to a two-dimensional electric potential problem on the molecular surface. In the following we only show the main results and the details are presented in the Appendices.

Define $F(\mathbf{r};\mathbf{s})=\frac{1}{\epsilon_s|\mathbf{r}-\mathbf{s}|}$ and $P(\mathbf{r};\mathbf{s})=\sum_{l=1,2}C_l\frac{e^{-k_l|\mathbf{r}-\mathbf{s}|}}{\epsilon_s|\mathbf{r}-\mathbf{s}|}$, $k_{1,2}=\frac{\sqrt{(1\mp\sqrt{1-4\kappa^2L_Q^2})/2}}{L_Q}$ and $C_{1,2}=\pm\frac{k_1^2+k_2^2}{k_2^2-k_1^2}$, where k_1,k_2 are from the first two roots of the bulk solvent dielectric function. The main working equations read

$$\frac{\psi(\mathbf{r}_0)}{2}=\oint_\Sigma\left[F(\mathbf{r};\mathbf{r}_0)\frac{\partial\psi(\mathbf{r})}{\partial n}-\psi(\mathbf{r})\frac{\partial F(\mathbf{r};\mathbf{r}_0)}{\partial n}\right]dS+\sum_{j=1}^{N}q_jF(\mathbf{r}_j;\mathbf{r}_0), \tag{6}$$

$$\begin{aligned}\frac{\psi(\mathbf{r}_0)}{2}&=\oint_\Sigma\left[-P(\mathbf{r};\mathbf{r}_0)\frac{\partial\psi(\mathbf{r})}{\partial n}+\psi(\mathbf{r})\frac{\partial P(\mathbf{r};\mathbf{r}_0)}{\partial n}\right]dS\\ &+\oint_\Sigma L_Q^2\left[\nabla^2P(\mathbf{r};\mathbf{r}_0)\frac{\partial\psi(\mathbf{r})}{\partial n}-\psi(\mathbf{r})\frac{\partial\nabla^2P(\mathbf{r};\mathbf{r}_0)}{\partial n}-\psi(\mathbf{r})\frac{\partial P(\mathbf{r};\mathbf{r}_0)}{\partial n}\right]dS,\end{aligned} \tag{7}$$

$$\frac{\nabla^2\psi(\mathbf{r}_0)}{2}=\oint_\Sigma\left[\kappa^2\left(\psi(\mathbf{r})\frac{\partial P(\mathbf{r};\mathbf{r}_0)}{\partial n}-P(\mathbf{r};\mathbf{r}_0)\frac{\partial\psi(\mathbf{r})}{\partial n}\right)-L_Q^2\nabla^2\psi(\mathbf{r})\frac{\partial\nabla^2P(\mathbf{r};\mathbf{r}_0)}{\partial n}\right]dS. \tag{8}$$

Eqs.(6), (7) and (8) are linear integral equations for three variables $\psi(\mathbf{r}_0)$, $\frac{\partial\psi(\mathbf{r}_0)}{\partial n}$ and $\nabla^2\psi(\mathbf{r}_0)$. When the third boundary condition Eq.(5) is replaced by other ones such as the continuity of $\frac{\partial^3\psi(\mathbf{r})}{\partial n^3}$ as in Ref.47 or the continuity of component Q_{nn} of the quadrupolarization tensor $\mathbf{Q}$ as in Ref.45, it would be hard to find a set of closed linear equations for the three functions $\psi(\mathbf{r}_0)$, $\frac{\partial\psi(\mathbf{r}_0)}{\partial n}$ and $\nabla^2\psi(\mathbf{r}_0)$ due to the fact that it is nontrivial to expand $\frac{\partial^3\psi(\mathbf{r})}{n^3}$ or Q_{nn} as a linear combination of $\psi(\mathbf{r}_0)$, $\frac{\partial\psi(\mathbf{r}_0)}{\partial n}$ and $\nabla^2\psi(\mathbf{r}_0)$. To this end, the boundary conditions used in this study may be the simplest one that supports the boundary element method.

In general, the three functions $\psi(\mathbf{r}_0)$, $\frac{\partial\psi(\mathbf{r}_0)}{\partial n}$ and $\nabla^2\psi(\mathbf{r}_0)$ can be solved numerically for a solute with general geometry and charge distribution using similar methodology as the conventional boundary element method.[14,20] When $\psi(\mathbf{r}_0)$, $\frac{\partial\psi(\mathbf{r}_0)}{\partial n}$ and $\nabla^2\psi(\mathbf{r}_0)$ are determined, one can use Eq.(27) and Eq.(29) of section 5 to evaluate the inside electric potential $\phi(\mathbf{r}_-)$ and the outside electric potential $\psi(\mathbf{r}_+)$. $\phi(\mathbf{r}_-)$ can be rewritten as

$$\phi(\mathbf{r}_-) = \oint_\Sigma \left[F(\mathbf{r};\mathbf{r}_-)\frac{\partial\psi(\mathbf{r})}{\partial n} - \psi(\mathbf{r})\frac{\partial F(\mathbf{r};\mathbf{r}_-)}{\partial n} \right] dS + \sum_{i=1}^{N} q_i F(\mathbf{r}_i;\mathbf{r}_-). \tag{9}$$

The induced potential ϕ_j^{ind} at the site j of the solute reads

$$\phi_j^{ind} \equiv \lim_{\mathbf{r}_- \longrightarrow \mathbf{r}_j} \left[\phi(\mathbf{r}_-) - \sum_{i=1}^{N} q_i F(\mathbf{r}_i;\mathbf{r}_-) \right] = \oint_\Sigma \left[F(\mathbf{r};\mathbf{r}_j)\frac{\partial\psi(\mathbf{r})}{\partial n} - \psi(\mathbf{r})\frac{\partial F(\mathbf{r};\mathbf{r}_j)}{\partial n} \right] dS. \tag{10}$$

The excess electrostatic energy βu_e then can be evaluated as

$$\beta u_e = \sum_{j=1}^{N} \beta q_j \phi_j^{ind}. \tag{11}$$

Note that the induced potential depends linearly on the solute charge, hence the electrostatic part of the excess chemical potential $\beta\mu_e$ equals to the excess electrostatic energy βu_e,[33] i.e.,

$$\beta\mu_e = \beta u_e. \tag{12}$$

2.4 A prescription to determine the parameters of the EDH dielectric response model

As our current theory needs the input parameters κ and L_Q from a pure solvent's dielectric function, it is assumed that this information is known from other sources such as experiments or other theoretical calculations. For example, let $\epsilon_l(k)$ be the longitudinal dielectric function of the pure solvent, the dielectric response function $\chi(k) \equiv 1 - \frac{\epsilon_0}{\epsilon_l(k)}$ can be evaluated using radial distribution functions $g_{ij}(r)$ of the pure solvent, $\chi(k) = \frac{4\pi\beta n_s}{k^2}[\sum_{i=1,2} q_i^2 x_i + n_s \sum_{i,j=1,2} q_i q_j x_i x_j g_{ij}(k)]$, where $g_{ij}(k) = \int e^{-i\mathbf{k}\cdot\mathbf{r}} g_{ij}(r) d\mathbf{r}$ is the three dimensional Fourier transform of $g_{ij}(r)$, $q_{1,2} = \pm q_s$ and $x_{1,2} = \frac{1}{2}$ for a restricted primitive model of electrolyte solutions.[33] When $\chi(k)$ of the pure solvent is used as input, one can fit it to an empirical function $\chi(k) = \frac{a_0 k^2}{k^4 + (a_1 k^2 - a_2)\cos(kb) + a_3 \sin(kb) + a_2}$, and then the poles $k = ik_n$ can be determined by solving $k^4 + (a_1 k^2 - a_2)\cos(kb) + a_3 \sin(kb) + a_2 = 0$ numerically.[40] κ and L_Q are chosen as

$$\kappa = \sqrt{\frac{k_1^2 k_2^2}{k_1^2 + k_2^2}}, L_Q = \sqrt{\frac{1}{k_1^2 + k_2^2}}, \tag{13}$$

so that the bulk system can be approximately described by a response function using $k_{1,2}$ from Eq.(26). It is well known that $k_{1,2}$ are two real numbers for weak electrostatic coupling and become complex conjugate when the electrostatic coupling is strong. It is easy to check that κ and L_Q defined via Eq.(13) are always real numbers. As will be shown in the next subsection, such a choice could reproduce the same asymptotic electric potential as our molecular DH theory with two Debye modes.[33]

For a solute with a general geometrical shape and charge distribution, one can use Eqs.(6), (7) and (8) to find the electric potential on the surface and use Eq.(10) to find the induced electric potential at each site and then the electrostatic energy is evaluated with Eq.(11). Naturally, the electric potential problem can also be solved numerically by finite difference using the corresponding differential equations, Eqs.(1) and (2), but our focus of this work is on the development of the boundary element method using integral equations, which may

provide certain advantages for some problems.

When the electrostatic coupling is very strong, a large number of Debye lengths is necessary to capture the dielectric response of an electrolyte solution,[29,33] the nonlinear response may also play an important role,[51] but our general strategy is to use multiple linear modes and suitable linear coefficients to mimic the nonlinear effect. Although each mode is based on linear response, the linear coefficients could carry information beyond linear response. Such a strategy has been applied in our previous study on the property of electrolyte solutions.[33] As long as the coefficient of each mode is properly determined, our theory can lead to a good description of both the electrostatic energy and the induced charge density of the solvent ions. To this end, a theory with multiple linear modes and refined linear coefficients could at least partly capture the nonlinear effect. As our current EDH theory is a linear theory which only use two Debye lengths, one can expect that our theory would fail for electrolyte solutions with strong electrostatic coupling. One may also note other shortcomings of our theory due to the simplicity of our dielectric response model, for example, the application of our theory to various systems lead to results for $B_{1,2}$ that violate the Stillinger-Lovett second moment condition or the electrostatic energy of the bulk system is less accurate than some other theories of electrolyte solution.[33,37,52]

On the other hand, higher order gradient terms can be included in our model in a straightforward manner. For example, when terms such as $\nabla^6\psi(r)$ and $\nabla^8\psi(r)$ are added to the dielectric response model, the electric potential will be a combination of four Yukawa potentials. As long as the extended Green's theorems are used for the three dimensional integrals such as $\int_{\Omega_2} d\mathbf{r}[f(\mathbf{r})\nabla^6 g(\mathbf{r}) - g(\mathbf{r})\nabla^6 f(\mathbf{r})]$ and $\int_{\Omega_2} d\mathbf{r}[f(\mathbf{r})\nabla^8 g(\mathbf{r}) - g(\mathbf{r})\nabla^8 f(\mathbf{r})]$, it would also be possible to derive the corresponding integral equations for the boundary element method. To this end, our study paves the way to extend the DH theory in a systematic way by adding high order gradient terms to represent the existence of various length scales in the dielectric response.

2.5 Electrostatic potential for a spherical ion: an example of applications

As a demonstration of our current approach, let's consider the electric potential problem of a spherical ion, where analytical solution of the potential can be found. Assume that the radius of the excluded sphere is a, and a point charge q is located at the center of the sphere. Due to the spherical symmetry, functions $f(\mathbf{r}) = \phi(\mathbf{r}), \psi(\mathbf{r}), \nabla^2\psi(\mathbf{r})$ depend only on the radius variable $r = |\mathbf{r}|$, and the value of $f(\mathbf{r}_0)$ on the spherical surface is a constant.

After some straightforward but lengthy calculations, one can find the solution of Eqs. (37), Eq.(38) and Eq.(39) . The final results read

$$\phi(r) = \frac{q}{\epsilon_s r} - \frac{q}{\epsilon_s a}\left[1 - \frac{k_2^2}{(k_2^2 - k_1^2)(1 + k_1 a)} - \frac{k_1^2}{(k_1^2 - k_2^2)(1 + k_2 a)}\right], \tag{14}$$

$$\psi(r) = \frac{q}{\epsilon_s}\left[\frac{k_2^2}{(k_2^2 - k_1^2)}\frac{e^{-k_1(r-a)}}{(1 + k_1 a)r} + \frac{k_1^2}{(k_1^2 - k_2^2)}\frac{e^{-k_2(r-a)}}{(1 + k_2 a)r}\right]. \tag{15}$$

The interested readers could find more details in section 5.

It is also possible to solve the electric potential using the corresponding differential equations, Eqs.(1) and (2) if the following test solution is used [45]

$$\phi(r) = \frac{q}{\epsilon_s r} + A, r < a \tag{16}$$

$$\psi(r) = \frac{q}{\epsilon_s}\sum_{l=1,2}\frac{B_l e^{-k_l(r-a)}}{(1 + k_l a)r}, r > a. \tag{17}$$

One may note that the functional form of the above test solutions depends on the property of the Eq.(1) and Eq.(2) rather than the boundary conditions; but different boundary conditions will lead to different set of A and $B_{1,2}$,[45–47] thus different solutions.

When the boundary conditions Eqs.(3), (4)and (5) are used, one can find that

$$A = -\frac{q}{\epsilon_s}\sum_{l=1,2}\frac{B_l k_l}{1+k_l a}, \tag{18}$$

$$B_1 = \frac{k_2^2}{k_2^2 - k_1^2}, \tag{19}$$

$$B_2 = 1 - B_1 = \frac{k_1^2}{k_1^2 - k_2^2}. \tag{20}$$

It is easy to check that Eqs.(14) and (15) are the same as Eqs.(16) and (17) if Eqs.(18), (19) and (20) are used. It should be noted that this solution has the same functional form as our molecular Debye-Hückel theory with two Debye modes,[33] hence one may view the EDH theory as a possible extension of our molecular DH theory with a different way of determining the linear combination coefficients of various Debye modes. Due to the simplicity of our dielectric response model, the coefficients of tagged solvent ions may not satisfy some universal constraints such as the Stillinger-Lovett second condition. Specifically, the Stilliger-Lovett condition leads to a constraint $B_1 f(k_1) + B_2 f(k_2) = 1$ with $f(k_i) = \frac{\kappa_D^2}{k_i^2}\frac{1+k_i\sigma_s+k_i^2\sigma_s^2/2+k_i^3\sigma_s^3/6}{1+k_i\sigma_s}$,[33] from which a different $B_{1,2}$ can be found. It will be interesting to study possible boundary conditions which could lead to a self-consistent theory of the solvent without violating such universal constraints.

Using Eq.(11), the electrostatic energy βu_e of the ion reads

$$\beta u_e = \beta q A = -\frac{\beta q^2}{2\epsilon_s}\sum_{l=1,2}\frac{B_l k_l}{1+k_l a} = -\frac{\beta q^2}{2\epsilon_s}\frac{k_1 k_2}{(k_1+k_2)}\frac{1+(k_1+k_2)a}{(1+k_1 a)(1+k_2 a)}. \tag{21}$$

3 Results and Discussion

To demonstrate the validity of our EDH theory, we apply the theory to electrolyte solutions with moderate electrostatic coupling. Specifically we test our theory against the mean spherical approximation(MSA),[53] hyper-netted chain(HNC)approximation of electrolyte solutions, and a diatomic solute in an electrolyte solution where the excess internal energy βu_e

and the electrostatic part of the excess chemical potential $\beta\mu_e$ are known. As we focus on the electrostatic effect, we will only compare the electrostatic energy. It is shown that our EDH model are capable of predicting the electrostatic energy accurately even if the electrostatic coupling is moderate.

3.1 Tests against the mean spherical approximation of electrolyte solutions

As the first test case, we consider the mean spherical approximation(MSA)[53] for primitive models, which leads to analytical results for the dielectric function, excess energy and other excess thermodynamic properties. MSA theory is used as input to evaluate the response function $\chi(k)$ and from which one can find $k_{1,2}$. As the electrostatic part of the excess chemical potential $\beta\mu_e$ equals to the electrostatic energy βu_e according to the MSA theory, we will only show the results for the electrostatic energy.

Firstly, we consider the electrostatic energy of a pure solvent, namely a two-component electrolyte solution with parameters $q_s = 1$, $\epsilon_s = 1$, $\sigma_s = 1$ and $\beta = 4$. The Debye parameter is evaluated as $\kappa_D = \sqrt{\frac{4\pi\beta n_s q_s^2}{\epsilon_s}}$, where n_s is the total particle number density. Within the MSA theory, all the electrostatic contribution to the thermodynamic properties of the system depends on the dimensionless reduced Debye parameter $K_D \equiv \kappa_D\sigma_s$. For $0.0002 < n_s < 1.0$, we found $0.100 < K_D < 7.09$. The electrostatic energies βu_e of the solvent species as a function of the Debye parameter K_D are shown in Fig.1. As one can see, EDH theory is in very good agreement with the MSA theory as long as the electrostatic coupling is not too strong, namely in the tested range of $0.1 \leq K_D \leq 7.0$, the relative energy difference between the EDH theory and MSA theory is less than 7 percent. As a comparison, the results from conventional DH theory are also shown. DH is not reliable for electrolyte solutions with strong electrostatic coupling, where the difference between the DH theory and MSA can be as large as 26 percent for the system at $K_D = 7.0$.

Secondly, we tested the electrostatic energy βu_e for solutes with various sizes when the

electrostatic coupling is moderate. The solvent is a binary electrolyte with $q_{1,2} = \pm 1$, $\epsilon_s = 1$, $\sigma_{1,2} = 1$ and $\beta = 4$. The solute charge q is fixed at $q = 1$ and the solute-solvent size ratio $\gamma = \frac{\sigma_o}{\sigma_s}$ is used as a control parameter. The radius of the excluded sphere of the solute ion reads $a = \frac{\sigma_s + \sigma_o}{2}$. For the test case with $K_D = 2.0$, it is found that $k_{1,2} = 1.8870 \pm 1.8876i$. The electrostatic energies for $0.2 \leq \gamma \leq 10$ are shown in Fig.2(a). In this case, the energy difference between the EDH theory and MSA theory is about 1 to 4 percent, while the energy difference between the DH theory and MSA theory is about 3 to 17 percent. For the test case with $K_D = 5.0$, it is found that $k_{1,2} = 1.1570 \pm 3.1426i$. The electrostatic energies for $0.2 \leq \gamma \leq 10$ are shown in Fig.2(b). The energy difference between the EDH theory and MSA theory is about 2 to 4 percent, while the energy difference between the DH theory and MSA theory is about 5 to 34 percent. Thus one can see that our EDH theory works much better than the DH theory when compared with the MSA theory. For other conditions where the Debye parameter is not too large, similar results are found and are not shown here.

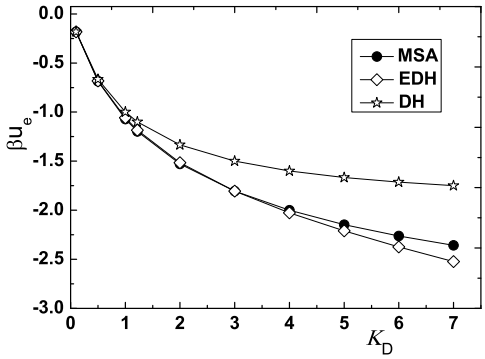

Figure 1: Electrostatic energy βu_e for pure solvents with various K_D. The results from MSA are denoted by filled circles, while our EDH theory and the DH theory are denoted by hollow diamonds and hollow stars. The lines are guides to the eye.

3.2 Test against HNC theory of electrolyte solutions

In this part we present the test of our theory against the HNC approximation, which is known to yield very accurate thermodynamic properties of primitive models.[53] The HNC

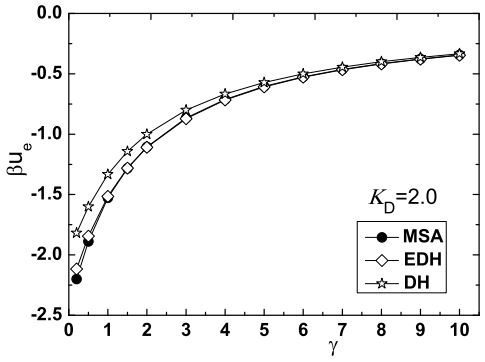

(a) The reduced Debye parameter of the solvent is $K_D = 2.0$.

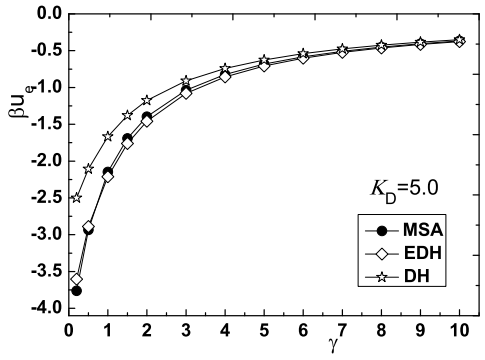

(b) The reduced Debye parameter of the solvent is $K_D = 5.0$.

Figure 2: Electrostatic energy βu_e as a function of the solute-solvent size ratio $\gamma = \frac{\sigma_o}{\sigma_s}$ under two solvent conditions. The results from MSA are denoted by filled circles, while our EDH theory and DH theory are denoted by hollow diamonds and hollow stars. The lines are guides to the eye.

theory is used as input to evaluate the response function $\chi(k)$ and from which one can find $k_{1,2}$. According to our previous study on the HNC theory,[33] the electrostatic part of the excess chemical potential $\beta\mu_e$ are in good agreement with the electrostatic energy βu_e, where the typical energy difference is about 1 percent as long as the electrostatic coupling is not too strong. So in the following we will not show the results for chemical potentials.

Firstly, we consider the electrostatic energy of a pure solvent. The parameters used for a binary electrolyte solvent are $q_s = 1$, $\epsilon_s = 1$, $\sigma_s = 1$, $\beta = 2$. We take the Debye parameter as the control parameter. For $0.005 \leq n_s \leq 0.8$, it is found that $0.354 \leq K_D \equiv k_D\sigma_s \leq 4.484$. The electrostatic energies βu_e for the solvent species are shown in Fig.3. Again, good agreement between our EDH theory and the HNC theory is found. The EDH theory differs from the HNC theory by 6 percent and 9 percent at reduced Debye parameter $K_D = 3.171$ and $K_D = 4.484$, while the DH theory overestimates the electrostatic energy by about 21 percent and 28 percent at $K_D = 3.171$ and $K_D = 4.484$.

Secondly, we consider the electrostatic energy of a solute with tunable sizes. The solvent parameters are fixed at $q_{1,2} = \pm 1$, $\epsilon_s = 1$, $\beta = 2$, $\sigma_{1,2} = \sigma_s = 1$. The solute charge is fixed at $q = 1$ and the solute-solvent size ratio $\gamma = \frac{\sigma_o}{\sigma_s}$ is used as a control parameter. For the test case with $n_s = 0.2$ where $K_D = 2.242$, it is found that $k_{1,2} = 1.9679 \pm 2.1439i$. The electrostatic energies for $0.2 \leq \gamma \leq 8$ are shown in Fig.4(a). The energy difference between the EDH theory and HNC theory is about 1 to 7 percent, while the energy difference between the DH theory and HNC theory is about 5 to 21 percent. For the test case with $n_s = 0.7$ where $K_D = 4.194$, it is found that $k_{1,2} = 1.6040 \pm 3.3280i$. The electrostatic energy for $0.2 \leq \gamma \leq 7$ are shown in Fig.4(b). The energy difference between the EDH theory and HNC theory is about 2 to 10 percent, while the energy difference between DH theory and HNC theory is about 9 to 31 percent. Again, our EDH theory shows a significant improvement over the DH theory. Our EDH theory is also tested for other conditions. As long as the reduced Debye parameter K_D and the solvent-solute size ratio are not too large, the EDH theory leads to satisfactory results compared with the HNC theory and is not shown. It is

worth to point out that $K_D = 4.0$ is equivalent to a $8.4M$ NaCl aqueous solution at room temperature, where the solvent parameters used are $\sigma_s = 4.2\mathring{A}$, $\epsilon_r = 78.5$, $T = 300K$.

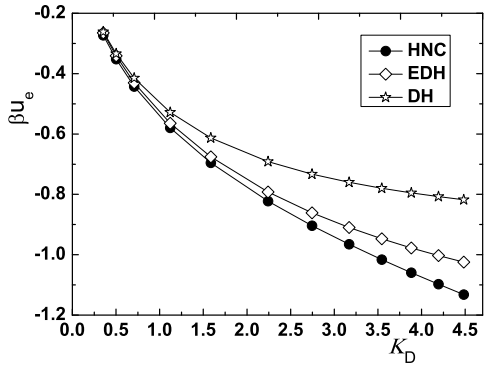

Figure 3: Excess electrostatic energies βu_e for pure solvent with various $K_D = \kappa_D \sigma_s$. The results from HNC are denoted by filled circles, while our EDH theory and DH theory are denoted by hollow diamonds and hollow stars. The lines are guides to the eye.

3.3 Test against molecular dynamics simulations of electrolyte solutions

In order to show that our theory is applicable to solutes beyond spherical geometry, we consider the electrostatic energy of a diatomic solute in a binary electrolyte solution. Denote $i = 1, 2$ as the cation and anion species of the binary electrolyte solvent. The charges of cations and anions are $q_{1,2} = \pm e_0$ with e_0 being the element charge, the temperature of the system is $T = 300K$, the permittivity of vacuum is ϵ_0, the relative dielectric constant of the back ground is $\epsilon_r = 78$, the total particle number density is $n_s = 0.007226\mathring{A}^{-3}$. Such a system is used to mimic a NaCl aqueous solution with salt concentration $c_0 = 6.00$ mol/L. The Debye parameter of the solution is about $\kappa_D = 0.805\mathring{A}^{-1}$. The non-electrostatic interaction between the solvent ions is a Lennard-Jones(LJ) potential $u_s(r) = 4\epsilon_s[(\frac{\sigma_s}{r})^{12} - (\frac{\sigma_s}{r})^6]$. The solute is a tagged diatomic molecule with two interaction sites denoted as j=3 and 4, where the charges of two sites are chosen to be q_3 and q_4. The non-electrostatic interaction between the solute site and solvent ions reads $u_{so}(r) = 4\epsilon_{so}[(\frac{\sigma_{so}}{r})^{12} - (\frac{\sigma_{so}}{r})^6]$. The LJ parameters used

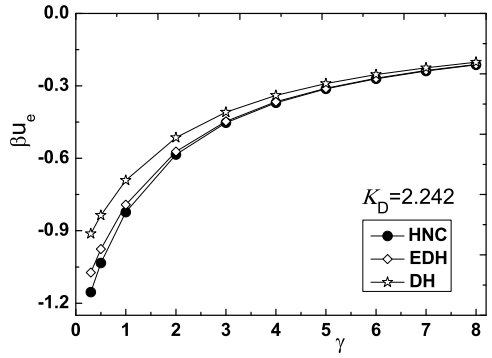

(a) The reduced Debye parameter of the solvent is $K_D = 2.242$.

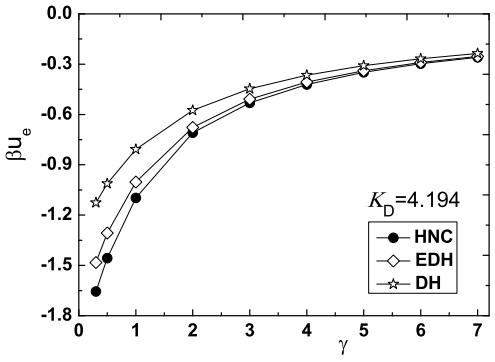

(b) The reduced Debye parameter of the solvent is $K_D = 4.194$.

Figure 4: Electrostatic energies βu_e as a function of the solute-solvent size ratio $\gamma = \frac{\sigma_o}{\sigma_s}$ under two solvent conditions. The results from HNC are denoted by filled circles, while our EDH theory and DH theory are denoted by hollow diamonds and hollow stars. The lines are guides to the eye.

are $\sigma_s = 3.5\mathring{A}$, $\epsilon_s = 1$ kJ/mol, $\sigma_{so} = 3.5\mathring{A}$ and ϵ_{so}=1 kJ/mol.

Molecular dynamics (MD) simulations are performed using the $DL-POLY$ program[54] with an NVT ensemble consisting of 216 ions in a cubic box with length $d = 31.0344\mathring{A}$. The time step used in the simulation is $\Delta t = 1.5$fs. The electrostatic energies u_e are calculated using the Ewald summation from equilibrium configurations, where the typical numerical uncertainty is below 0.04 kJ/mol for a total of 10^5 configuration. Using the radial distributions from the simulations, the dielectric response function $\chi(k)$ is calculated and then the first two Debye parameters are found to be $k_{1,2} = 0.5846 \pm 0.7673i$. The WCA prescription[55,56] is used to find the effective radius a of an ion or site, where $u_{12}(r) = u_s(r) + \frac{q_1 q_2}{\epsilon_0 \epsilon_r r}$ is used to compute the effective radius of the ions. The effective ion radius is found to be $a = 3.367\mathring{A}$ and is also used as the effective radius for each site of the diatomic molecule. Using our EDH theory, it is found that $B_{1,2} = 0.5 \pm 0.1377i$ for the ions and then the electrostatic energy for the solvent reads $u_e = -2.26$ kJ/mol which differs from the MD result $u_e = -2.41$ kJ/mol by 6 percent, while the DH theory leads to $u_e = -1.93$ kJ/mol which differs from the MD results by 20 percent.

In order to find the electrostatic energy of the diatomic solute, a total of 212 ions and two diatomic molecules are used for MD simulations. Two solutes have the same LJ potential but with opposite charge numbers so that the simulation box is neutral. The site separation distance R between site 3 and 4 in the diatomic solute is used as a control parameter. Each site of the diatomic molecule is mapped to a charged hard sphere with radius a and then the molecule is mapped to a union of charged hard spheres. In the case of large separations with $R > a$, a diatomic molecule is mapped to a system consisting of two individual spheres and then the electric potential could be solved with a two-center test solution.[40,57] In the case of small separations with $R < a$, hard spheres of the molecule sites are fused and then the diatomic molecules is dumbbell-shaped. As the diatomic solute have azimuthal symmetry, the electric potential depends on the radial variable r and an angle variable θ. When the site 3 is set at the origin, and the site 4 is set at $r = R$ and $\theta = 0$, one can

use the one-center test solution $\phi(r,\theta) = \frac{q_3}{\epsilon_0\epsilon_r r} + \frac{q_4}{\epsilon_0\epsilon_r\sqrt{r^2+R^2-2Rr\cos\theta}} + \sum_{n=0}^{N} A_n P_n(\cos\theta)$ and $\psi(r,\theta) = \sum_{n=0}^{N}[B_{1n}k_n(k_1 r)P_n(\cos\theta) + B_{2n}k_n(k_2 r)P_n(\cos\theta)]$ to compute the electric potential, where $P_n(x)$ is the Legendre Polynomial and $k_n(r)$ is the modified spherical Bessel function of the third kind.[40] When the three boundary conditions are used, a set of linear equation for variables $\{A_n\}$, $\{B_{1n}\}$ and $\{B_{2n}\}$ can be derived and can be solved numerically. The test solution method is also used to find the electric potential solution of the DH theory. In this study we focus on the case of small separations with $R \leq 3\mathring{A}$, where numerical calculation shows that $N = 9$ leads to converged results. For the charge distribution $q_{3,4} = e_0, 0$, the results for u_e in the range of $0.5\mathring{A} \leq R \leq 3\mathring{A}$ are shown in Fig.5(a). As one can see, the electrostatic energy of the solute only has a weak dependence on the site separation distance R. The energy difference between our EDH theory and the MD results is about 9 percent, while the energy difference between the DH theory and the MD results is about 22 percent. For the charge distribution $q_{3,4} = e_0, -e_0$, the results for u_e in the range of $0.5\mathring{A} \leq R \leq 3\mathring{A}$ are shown in Fig.5(b). In this case the electrostatic energy of the solute has a much stronger dependence on the site separation distance R. The energy difference between our EDH theory and the MD results is about 20 percent, while the energy difference between the DH theory and the MD results is more than 40 percent. In both cases one can see that our EDH theory works much better than the DH theory when applied to the diatomic solutes.

4 Conclusions

In summary, an extended Debye-Hückel theory with fourth order gradient term is developed for electrolyte solutions, where appropriate three boundary conditions are introduced based upon the continuity requirements of the involving functions at the boundary. The integral equations for the boundary element method are also derived, so that our theory is applicable to a solute with general geometrical shapes and charge distributions, but the numerical implementation will be left for future work. The electric potential as well as the electrostatic

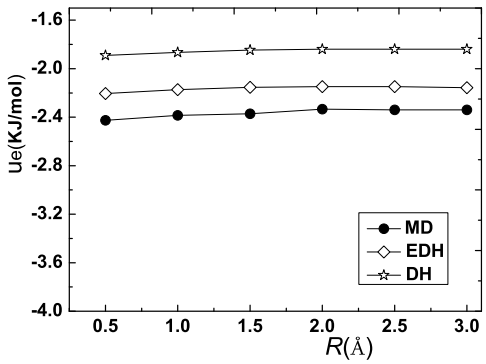

(a) The charges of the two sites are $q_{3,4} = e_0, 0$.

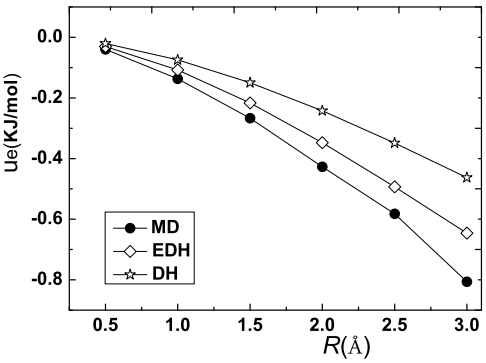

(b) The charges of the two sites are $q_{3,4} = e_0, -e_0$.

Figure 5: Excess electrostatic energies u_e for a diatomic molecule with various site separation distance R. The results from MD are denoted by filled circles, while our EDH theory and DH theory are denoted by hollow diamonds and hollow stars. The lines are guides to the eye.

energy are obtained for spherical ions and diatomic solutes where the validity of our theory is successfully demonstrated for binary as well as multi-component models of electrolyte solutions.

ACKNOWLEDGMENTS

T. Xiao acknowledges the financial support from the National Natural Science Foundation of China(NSFC)(Grant No. 21863001), and a startup package from Guizhou Education University. X. Song is supported by the Division of Chemical and Biological Sciences, Office of Basic Energy Sciences, U.S. Department of Energy, under Contract No. DE-AC02-07CH11358 with Iowa State University.

5 Appendices

5.1 Derivation of the Integral equations for the boundary element method

In this part we use Juffer *et al*'s prescription[14] to formulate a boundary element method for systems described by Eqs.(1) and (2). For the Poisson equation

$$\nabla^2 F(\mathbf{r};\mathbf{s}) = -\frac{4\pi}{\epsilon_s}\delta^{(3)}(\mathbf{r}-\mathbf{s}), \tag{22}$$

where $\delta^{(3)}(\mathbf{r})$ is the Dirac delta function, one can find the Green function

$$F(\mathbf{r};\mathbf{s}) = \frac{1}{\epsilon_s|\mathbf{r}-\mathbf{s}|}. \tag{23}$$

For a dielectric response equation with quadruple effect,

$$\nabla^2 P(\mathbf{r};\mathbf{s}) = \kappa^2 P(\mathbf{r};\mathbf{s}) + L_Q^2\nabla^4 P(\mathbf{r};\mathbf{s}) - \frac{4\pi}{\epsilon_s}\delta^{(3)}(\mathbf{r}-\mathbf{s}), \tag{24}$$

the Green function reads

$$P(\mathbf{r};\mathbf{s}) = \sum_{l=1,2} C_l \frac{e^{-k_l|\mathbf{r}-\mathbf{s}|}}{\epsilon_s|\mathbf{r}-\mathbf{s}|}, \tag{25}$$

where the Debye parameters $k_{1,2}$ and $C_{1,2}$ read

$$k_{1,2} = \frac{\sqrt{(1 \mp \sqrt{1-4\kappa^2 L_Q^2})/2}}{L_Q}, C_{1,2} = \pm\frac{k_1^2+k_2^2}{k_2^2-k_1^2}. \tag{26}$$

Using these two Green functions $F(\mathbf{r};\mathbf{s})$ and $P(\mathbf{r};\mathbf{s})$, the integral equations for the boundary element method can be derived.

Denote $\mathbf{r}_-$ as a point inside the solute, $\mathbf{r}_+$ as a point outside the solute, $\mathbf{r}_0$ as a point on the molecular surface. Multiplying $\phi(\mathbf{r}_-)$ with Eq.(22) and subtracting $F(\mathbf{r};\mathbf{r}_-)$ times Eq.(1), and using Green's second theorem for scalar functions $\int_{\Omega_1} d\mathbf{r}[f(\mathbf{r})\nabla^2 g(\mathbf{r}) - g(\mathbf{r})\nabla^2 f(\mathbf{r})] = \oint_\Sigma [f(\mathbf{r})\frac{\partial g(\mathbf{r})}{\partial n} - g(\mathbf{r})\frac{\partial f(\mathbf{r})}{\partial n}]dS$ on the volume inside Σ, one can find the following expression for $\phi(\mathbf{r}_-)$[14]

$$\phi(\mathbf{r}_-) = \oint_\Sigma \left[F(\mathbf{r};\mathbf{r}_-)\frac{\partial\phi(\mathbf{r})}{\partial n} - \phi(\mathbf{r})\frac{\partial F(\mathbf{r};\mathbf{r}_-)}{\partial n}\right] dS + \sum_{j=1}^{N} q_j F(\mathbf{r}_j;\mathbf{r}_-). \tag{27}$$

In order to find the integral equation for $\psi(\mathbf{r})$, we use an extended Green theorem for scalar functions $f(\mathbf{r})$ and $g(\mathbf{r})$,

$$\begin{aligned}\int_{\Omega_2} d\mathbf{r}[f(\mathbf{r})\nabla^4 g(\mathbf{r}) - g(\mathbf{r})\nabla^4 f(\mathbf{r})] = &-\oint_\Sigma \left[f(\mathbf{r})\frac{\partial\nabla^2 g(\mathbf{r})}{\partial n} - g(\mathbf{r})\frac{\partial\nabla^2 f(\mathbf{r})}{\partial n}\right] dS \\ &-\oint_\Sigma \left[\nabla^2 f(\mathbf{r})\frac{\partial g(\mathbf{r})}{\partial n} - \nabla^2 g(\mathbf{r})\frac{\partial f(\mathbf{r})}{\partial n}\right] dS,\end{aligned} \tag{28}$$

which can be viewed as generalized integration by parts.[58] Multiplying $\psi(\mathbf{r}_+)$ with Eq.(24) and subtracting $P(\mathbf{r};\mathbf{r}_+)$ times Eq.(2) and use the extended Green theorem Eq.(28) on the

volume outside Σ, one can find that

$$\begin{aligned}\psi(\mathbf{r}_+) = &\oint_\Sigma \left[-P(\mathbf{r};\mathbf{r}_+)\frac{\partial\psi(\mathbf{r})}{\partial n} + \psi(\mathbf{r})\frac{\partial P(\mathbf{r};\mathbf{r}_+)}{\partial n}\right] dS \\ &+ \oint_\Sigma L_Q^2 \left[P(\mathbf{r};\mathbf{r}_+)\frac{\partial\nabla^2\psi(\mathbf{r})}{\partial n} - \nabla^2\psi(\mathbf{r})\frac{\partial P(\mathbf{r};\mathbf{r}_+)}{\partial n}\right] dS \\ &+ \oint_\Sigma L_Q^2 \left[\nabla^2 P(\mathbf{r};\mathbf{r}_+)\frac{\partial\psi(\mathbf{r})}{\partial n} - \psi(\mathbf{r})\frac{\partial\nabla^2 P(\mathbf{r};\mathbf{r}_+)}{\partial n}\right] dS.\end{aligned} \tag{29}$$

The integral equation for $\nabla^2\psi(\mathbf{r})$ can also be found in a similar way. Multiplying $\nabla^2\psi(\mathbf{r})$ with Eq.(24) and subtracting $\nabla^2 P(\mathbf{r};\mathbf{r}_+)$ times Eq.(2) and use the Green theorem and the extended Green theorem Eq.(28) on the volume outside Σ, one can find that

$$\begin{aligned}\nabla^2\psi(\mathbf{r}_+) = &\oint_\Sigma \kappa^2 \left[\psi(\mathbf{r})\frac{\partial P(\mathbf{r};\mathbf{r}_+)}{\partial n} - P(\mathbf{r};\mathbf{r}_+)\frac{\partial\psi(\mathbf{r})}{\partial n}\right] dS \\ &+ \oint_\Sigma L_Q^2 \left[\nabla^2 P(\mathbf{r};\mathbf{r}_+)\frac{\partial\nabla^2\psi(\mathbf{r})}{\partial n} - \nabla^2\psi(\mathbf{r})\frac{\partial\nabla^2 P(\mathbf{r};\mathbf{r}_+)}{\partial n}\right] dS.\end{aligned} \tag{30}$$

In order to find a solution of the electric potential problem, we need to find the electric potential on the molecular surface. Using the properties of single layer and double layer integral,[59] it is found that

$$\phi(\mathbf{r}_0) \equiv \lim_{\mathbf{r}_-\to\mathbf{r}_0}\phi(\mathbf{r}_-) = \oint_\Sigma \left[F(\mathbf{r};\mathbf{r}_0)\frac{\partial\phi(\mathbf{r})}{\partial n} - \phi(\mathbf{r})\frac{\partial F(\mathbf{r};\mathbf{r}_0)}{\partial n}\right] dS + \sum_{j=1}^{N} q_j F(\mathbf{r}_j;\mathbf{r}_0) + \frac{\phi(\mathbf{r}_0)}{2}, \tag{31}$$

$$\begin{aligned}\psi(\mathbf{r}_0) \equiv \lim_{\mathbf{r}_+\to\mathbf{r}_0}\psi(\mathbf{r}_+) = &\oint_\Sigma \left[-P(\mathbf{r};\mathbf{r}_0)\frac{\partial\psi(\mathbf{r})}{\partial n} + \psi(\mathbf{r})\frac{\partial P(\mathbf{r};\mathbf{r}_0)}{\partial n}\right] dS \\ &+ \oint_\Sigma L_Q^2 \left[P(\mathbf{r};\mathbf{r}_0)\frac{\partial\nabla^2\psi(\mathbf{r})}{\partial n} - \nabla^2\psi(\mathbf{r})\frac{\partial P(\mathbf{r};\mathbf{r}_0)}{\partial n}\right] dS \\ &+ \oint_\Sigma L_Q^2 \left[\nabla^2 P(\mathbf{r};\mathbf{r}_0)\frac{\partial\psi(\mathbf{r})}{\partial n} - \psi(\mathbf{r})\frac{\partial\nabla^2 P(\mathbf{r};\mathbf{r}_0)}{\partial n}\right] dS + \frac{\psi(\mathbf{r}_0)}{2},\end{aligned} \tag{32}$$

$$\begin{aligned}\nabla^2\psi(\mathbf{r}_0) \equiv \lim_{\mathbf{r}_+\to\mathbf{r}_0}\nabla^2\psi(\mathbf{r}_+) = &\oint_\Sigma \kappa^2 \left[\Psi(\mathbf{r})\frac{\partial P(\mathbf{r};\mathbf{r}_0)}{\partial n} - P(\mathbf{r};\mathbf{r}_0)\frac{\partial\psi(\mathbf{r})}{\partial n}\right] dS \\ &+ L_Q^2 \left[\nabla^2 P(\mathbf{r};\mathbf{r}_0)\frac{\partial\nabla^2\psi(\mathbf{r})}{\partial n} - \nabla^2\psi(\mathbf{r})\frac{\partial\nabla^2 P(\mathbf{r};\mathbf{r}_0)}{\partial n}\right] dS + \frac{\nabla^2\psi(\mathbf{r}_0)}{2}.\end{aligned} \tag{33}$$

As the boundary conditions Eqs.(3),(4) and (5)reduce to

$$\psi(\mathbf{r}_0) = \phi(\mathbf{r}_0), \tag{34}$$

$$\frac{\partial\psi(\mathbf{r}_0)}{\partial n} = \frac{\partial\phi(\mathbf{r}_0)}{\partial n}, \tag{35}$$

$$\frac{\partial\nabla^2\psi(\mathbf{r}_0)}{\partial n} = \frac{\partial\nabla^2\phi(\mathbf{r}_0)}{\partial n} \equiv 0; \tag{36}$$

Eqs.(31), (32) and (33) reduce to

$$\frac{\psi(\mathbf{r}_0)}{2} = \oint_\Sigma \left[F(\mathbf{r};\mathbf{r}_0)\frac{\partial\psi(\mathbf{r})}{\partial n} - \psi(\mathbf{r})\frac{\partial F(\mathbf{r};\mathbf{r}_0)}{\partial n} \right] dS + \sum_{j=1}^{N} q_j F(\mathbf{r}_j;\mathbf{r}_0), \tag{37}$$

$$\begin{aligned} \frac{\psi(\mathbf{r}_0)}{2} &= \oint_\Sigma \left[-P(\mathbf{r};\mathbf{r}_0)\frac{\partial\psi(\mathbf{r})}{\partial n} + \psi(\mathbf{r})\frac{\partial P(\mathbf{r};\mathbf{r}_0)}{\partial n} \right] dS \\ - \oint_\Sigma L_Q^2 \left[\nabla^2 P(\mathbf{r};\mathbf{r}_0)\frac{\partial\psi(\mathbf{r})}{\partial n} - \psi(\mathbf{r})\frac{\partial\nabla^2 P(\mathbf{r};\mathbf{r}_0)}{\partial n} - \nabla^2\psi(\mathbf{r})\frac{\partial P(\mathbf{r};\mathbf{r}_0)}{\partial n} \right] dS, \end{aligned} \tag{38}$$

$$\frac{\nabla^2\psi(\mathbf{r}_0)}{2} = \oint_\Sigma \left[\kappa^2 \left(\psi(\mathbf{r})\frac{\partial P(\mathbf{r};\mathbf{r}_0)}{\partial n} - P(\mathbf{r};\mathbf{r}_0)\frac{\partial\psi(\mathbf{r})}{\partial n} \right) - L_Q^2\nabla^2\psi(\mathbf{r})\frac{\partial\nabla^2 P(\mathbf{r};\mathbf{r}_0)}{\partial n} \right] dS. \tag{39}$$

The above three equations are the main working equations for the boundary element method. Once $\psi(\mathbf{r}_0)$, $\frac{\partial\psi(\mathbf{r}_0)}{\partial n}$ and $\nabla^2\psi(\mathbf{r}_0)$ are determined with Eq.(37), Eq.(38) and Eq.(39), one can use Eq.(27) and Eq.(29) to evaluate the inside electric potential $\phi(\mathbf{r}_-)$ and the outside electric potential $\psi(\mathbf{r}_+)$.

5.2 Derivation of the electric potential of a spherical ion

We show how to find the solution of Eq.(37), Eq.(38) and Eq.(39) given the solute is a spherical ion. Due to the spherical symmetry, we introduce $\psi(\mathbf{r}_0) \equiv \psi_s$, $\frac{\partial\psi(\mathbf{r}_0)}{\partial n} \equiv h_s$, $\nabla^2\psi(\mathbf{r}_0) \equiv u_s$,

then Eqs.(37) , (38) and (39) reduce to

$$\frac{\psi_s}{2} = \oint \left[F(\mathbf{r};\mathbf{r}_0) h_s - \psi_s \frac{\partial F(\mathbf{r};\mathbf{r}_0)}{\partial n} \right] dS + \frac{q}{\epsilon_s a}, \tag{40}$$

$$\frac{\psi_s}{2} = \oint \left[-P(\mathbf{r};\mathbf{r}_0) h_s + \psi_s \frac{\partial P(\mathbf{r};\mathbf{r}_0)}{\partial n} + L_Q^2 \left(\nabla^2 P(\mathbf{r};\mathbf{r}_0) h_s - \psi_s \frac{\partial \nabla^2 P(\mathbf{r};\mathbf{r}_0)}{\partial n} - u_s \frac{\partial P(\mathbf{r};\mathbf{r}_0)}{\partial n} \right) \right] dS, \tag{41}$$

$$\frac{u_s}{2} = \oint \left[\kappa^2 \left(\psi_s \frac{\partial P(\mathbf{r};\mathbf{r}_0)}{\partial n} - P(\mathbf{r};\mathbf{r}_0) h_s \right) - L_Q^2 \nabla^2 \psi_s \frac{\partial \nabla^2 P(\mathbf{r};\mathbf{r}_0)}{\partial n} \right] dS. \tag{42}$$

Using $I_1 \equiv \oint F(\mathbf{r};\mathbf{r}_0) dS = a$, $I_2 \equiv \oint \frac{\partial F(\mathbf{r};\mathbf{r}_0)}{\partial n} dS = -\frac{1}{2}$, $I_3 \equiv \oint P(\mathbf{r};\mathbf{r}_0) dS = \sum_{l=1,2} \frac{C_l(1-e^{-2k_l a})}{2k_l}$, $I_4 \equiv \oint \frac{\partial P(\mathbf{r};\mathbf{r}_0)}{\partial n} dS = \sum_{l=1,2} \frac{C_l[1-(1+k_l a)e^{-2k_l a}]}{-2k_l a}$, $I_5 \equiv \oint \nabla^2 P(\mathbf{r};\mathbf{r}_0) dS = \sum_{l=1,2} \frac{C_l k_l (1-e^{-2k_l a})}{2}$, $I_6 \equiv \oint \frac{\partial \nabla^2 P(\mathbf{r};\mathbf{r}_0)}{\partial n} dS = \sum_{l=1,2} \frac{C_l k_l [1-(1+k_l a)e^{-2k_l a}]}{-2a}$, one can find that

$$\psi_s = \frac{q}{\epsilon_s a} \frac{k_1 + k_2 + (k_1^2 + k_2^2 + k_1 k_2) a}{(k_1 + k_2)(1 + k_1 a)(1 + k_2 a)}, \tag{43}$$

$$h_s = -\frac{q}{\epsilon_s a^2}, \tag{44}$$

$$u_s = \frac{q}{\epsilon_s} \frac{k_1^2 k_2^2}{(k_1 + k_2)(1 + k_1 a)(1 + k_2 a)}. \tag{45}$$

Using Eqs.(43), (44) and (45), one can use Eqs.(27) and (29) to evaluate the electric potential $\phi(\mathbf{r}) = \phi(r)$ and $\psi(\mathbf{r}) = \psi(r)$. After some straightforward but tedious calculations, the final results read

$$\phi(r) = \frac{q}{\epsilon_s r} - \frac{q}{\epsilon_s a} \left[1 - \frac{k_2^2}{(k_2^2 - k_1^2)(1 + k_1 a)} - \frac{k_1^2}{(k_1^2 - k_2^2)(1 + k_2 a)} \right], \tag{46}$$

$$\psi(r) = \frac{q}{\epsilon_s} \left[\frac{k_2^2}{(k_2^2 - k_1^2)} \frac{e^{-k_1(r-a)}}{(1 + k_1 a) r} + \frac{k_1^2}{(k_1^2 - k_2^2)} \frac{e^{-k_2(r-a)}}{(1 + k_2 a) r} \right]. \tag{47}$$

References

(1) Simonson,; Thomas, Electrostatics and dynamics of proteins. *Rep. Prog. Phys.* **2003**, *66*, 737–787.

(2) Mennucci, B.; Cammi, R.; Interscience, W. *Continuum solvation models in chemical physics: from theory to applications*; Wiley Online Library, 2007.

(3) Chayen, N. E.; Saridakis, E. Protein crystallization: from purified protein to diffraction-quality crystal. *Nat. Methods* **2008**, *5*, 147–153.

(4) Holst, M.; Kozack, R. E.; Saied, F.; Subramaniam, S. Treatment of electrostatic effects in proteins: multigrid-based Newton iterative method for solution of the full nonlinear Poisson-Boltzmann equation. *Proteins* **2010**, *18*, 231–245.

(5) Collins, K. D.; Washabaugh, M. W. The Hofmeister effect and the behaviour of water at interfaces. *Q. Rev. Biophys.* **1985**, *18*, 323–422.

(6) Ninham, B. W.; Yaminsky, V. Ion Binding and Ion Specificity: The Hofmeister Effect and Onsager and Lifshitz Theories. *Langmuir* **1997**, *13*, 2097–2108.

(7) Bhuiyan, L. B.; Bratko, D.; Outhwaite, C. W. Electrolyte surface tension in the modified Poisson-Boltzmann approximation. *J. Phys. Chem.* **2002**, *95*, 336–340.

(8) Levin, Y. Thermodynamics of surface tension: Application to electrolyte solutions. *J. Stat. Phys.* **2003**, *110*, 825–834.

(9) Marcus, R. Chemical and electrochemical electron-transfer theory. *Ann. Rev. Phys. Chem.* **1964**, *15*, 155–196.

(10) Hwang, J. K.; Warshel, A. MICROSCOPIC EXAMINATION OF FREE-ENERGY RELATIONSHIPS FOR ELECTRON-TRANSFER IN POLAR-SOLVENTS. *J. Am. Chem. Soc.* **1987**, *109*, 715–720.

(11) Newton, M. D.; Sutin, N. Electron transfer reactions in condensed phases. *Ann. Rev. Phys. Chem.* **1984**, *35*, 437–480.

(12) Blumberger, J.; Sprik, M. In *Computer Simulations in Condensed Matter Systems: From Materials to Chemical Biology, Vol 2*; Ferrariao, M., Ciccotti, G., Binder, K., Eds.; Lecture Notes in Physics; Springer: Heidelberg, 2006; Vol. 704; pp 481–506.

(13) Debye, P.; Hückel, E. The theory of electrolytes I. The lowering of the freezing point and related occurrences. *Zeit. Für Phys.* **1923**, *24*, 185–206.

(14) Juffer, A. H.; Botta, E. F. F.; Keulen, B. A. M. V.; Ploeg, A. V. D.; Berendsen, H. J. C. The electric potential of a macromolecule in a solvent: A fundamental approach. *J. Comput. Phys.* **1991**, *97*, 144–171.

(15) Zhou, H. X. Boundary element solution of macromolecular electrostatics: interaction energy between two proteins. *Biophys. J.* **1993**, *65*, 955–963.

(16) Liang, J.; Subramaniam, S. Computation of molecular electrostatics with boundary element methods. *Biophys. J.* **1997**, *73*, 1830 – 1841.

(17) Totrov, M.; Abagyan, R. Rapid boundary element solvation electrostatics calculations in folding simulations: Successful folding of a 23-residue peptide. *Peptide Sci.* **2015**, *60*, 124–133.

(18) Vorobjev, Y. N.; Scheraga, H. A. A fast adaptive multigrid boundary element method for macromolecular electrostatic computations in a solvent. *J. Comput. Chem.* **2015**, *18*, 569–583.

(19) Bardhan, J. P. *Boundary-Integral and Boundary-Element Methods for Biomolecular Electrostatics: Progress, Challenges, and Important Lessons from CEBA 2013*; 2015.

(20) Kim, B.; Song, X. Y. Calculations of the second virial coefficients of protein solutions with an extended fast multipole method. *Phys. Rev. E* **2011**, *83*, 011915/1–011915/15.

(21) Varela, L. M.; Garcia, M.; Mosquera, V. Exact mean-field theory of ionic solutions: non-Debye screening. *Phys. Rep.* **2003**, *382*, 1–111.

(22) Kirkwood, J. G.; Poirier, J. C. The Statistical Mechanical Basis of the Debye–Hüekel Theory of Strong Electrolytes. *J. Chem. Phys.* **1954**, *58*, 591–596.

(23) Outhwaite, C. W. Extension of the Debye-Hückel Theory of Electrolyte Solutions. *J. Chem. Phys.* **1969**, *50*, 2277–2288.

(24) Outhwaite, C. W. The linear extension of the Debye-Hückel theory of electrolyte solutions. *Chem. Phys. Lett.* **1970**, *5*, 77–79.

(25) Outhwaite, C. W. A modified Poisson-Boltzmann approach to homogeneous ionic solutions. *Condens. Matter. Phys.* **2004**, *7*, 719–733.

(26) Stillinger, F. H.; Lovett, R. General restriction on the distribution of ions in electrolytes. *J. Chem. Phys.* **1968**, *49*, 1991–1994.

(27) Hansen, J. P.; McDonald, I. R. *Theory of simple liquids*; Academic: London, 1986.

(28) Naji, A.; Kanduc, M.; Forsman, J.; Podgornik, R. Perspective: Coulomb fluids – weak coupling, strong coupling, in between and beyond. *J. Chem. Phys.* **2013**, *139*, 1887–365.

(29) Kjellander, R.; Mitchell, D. J. Dressed-Ion Theory for Electrolyte-Solutions - a Debye-Hückel-Like Reformulation of the Exact Theory for the Primitive Model. *J. Chem. Phys.* **1994**, *101*, 603–626.

(30) Kjellander, R. Modified Debye-Hückel Approximation with Effective Charges - an Application of Dressed Ion Theory for Electrolyte-Solutions. *J. Phys. Chem.* **1995**, *99*, 10392–10407.

(31) Ulander, J.; Greberg, H.; Kjellander, R. Primary and secondary effective charges for electrical double layer systems with asymmetric electrolytes. *J. Chem. Phys.* **2001**, *115*, 7144–7160.

(32) Song, X. Solvation dynamics in ionic fluids: An extended Debye-Hüeckel dielectric continuum model. *J. Chem. Phys.* **2009**, *131*, 044503.

(33) Xiao, T.; Song, X. A molecular Debye-Hückel theory and its applications to electrolyte solutions. *J. Chem. Phys.* **2011**, *135*, 104104.

(34) Lee, B. P.; Fisher, M. E. Density Fluctuations in an Electrolyte from Generalized Debye-Hückel Theory. *Phys. Rev. Lett.* **1996**, *76*, 2906–2909.

(35) Keblinski, P.; Eggebrecht, J.; Wolf, D.; Phillpot, S. R. Molecular dynamics study of screening in ionic fluids. *J. Chem. Phys.* **2000**, *113*, 282–291.

(36) Coupette, F.; Lee, A. A.; Haertel, A. Screening lengths in ionic fluids. *Phys. Rev. Lett.* **2018**, *121*, 075501.

(37) Kjellander, R. A multiple decay-length extension of the Debye-Hückel theory: to achieve high accuracy also for concentrated solutions and explain under-screening in dilute symmetric electrolytes. *Phys. Chem. Chem. Phys.* **2020**, *22*, 23952–23985.

(38) Smith, A. M.; Lee, A. A.; Perkin, S. The Electrostatic Screening Length in Concentrated Electrolytes Increases with Concentration. *J. Phys. Chem. Lett.* **2016**, *7*, 2157–2163.

(39) Lee, A. A.; Perez-Martinez, C. S.; Smith, A. M.; Perkin, S. Scaling Analysis of the Screening Length in Concentrated Electrolytes. *Phys. Rev. Lett.* **2017**, *119*, 026002.

(40) Xiao, T.; Song, X. Reorganization energy of electron transfer processes in ionic fluids: a molecular Debye-Hückel approach. *J. Chem. Phys.* **2013**, *138*, 114105.

(41) Xiao, T.; Song, X. A molecular Debye-Hückel approach to the reorganization energy of electron transfer reactions in an electric cell. *J. Chem. Phys.* **2014**, *141*, 134104.

(42) Xiao, T. Extended Debye–Hückel Theory for Studying the Electrostatic Solvation Energy. *ChemPhysChem* **2015**, *16*, 833–841.

(43) Xiao, T. An analytical longitudinal dielectric function of primitive electrolyte solutions and its application in predicting thermodynamic properties. *Electrochim. Acta* **2015**, *178*, 101–107.

(44) Xiao, T.; Song, X. A molecular Debye-Hückel theory and its applications to electrolyte solutions: The size asymmetric case. *J. Chem. Phys.* **2017**, *146*, 124118.

(45) Slavchov, R. I. Quadrupole terms in the Maxwell equations: Debye-Hückel theory in quadrupolarizable solvent and self-salting-out of electrolytes. *J. Chem. Phys.* **2014**, *140*, 164510.

(46) Shirish, M. C. A continuum solvation theory of quadrupolar fluids. *J. Chem. Phys.* **1996**, *104*, 9065–9074.

(47) Jeon, J.; Kim, H. J. A continuum theory of solvation in quadrupolar solvents. I. Formulation. *J. Chem. Phys.* **2003**, *119*, 8606–8625.

(48) Slavchov, R. I.; Ivanov, T. I. Quadrupole terms in the Maxwell equations: Born energy, partial molar volume, and entropy of ions. *J. Chem. Phys.* **2014**, *140*, 074503.

(49) Slavchov, R. I.; Dimitrova, I. M.; Ivanov, T. The polarized interface between quadrupolar insulators: Maxwell stress tensor, surface tension, and potential. *J. Chem. Phys.* **2015**, *143*, 154707.

(50) Stakgold, I.; Holst, M. *Green's Functions and Boundary Value Problems, Third Edition*; John Wiley & Sons, 2011.

(51) Fisher, M. E.; Levin, Y. Criticality in ionic fluids: Debye-Hückel theory, Bjerrum, and beyond. *Phys. Rev. Lett.* **1993**, *71*, 3826–3829.

(52) Outhwaite, C. W.; Bhuiyan, L. B. Comments on the linear modified Poisson-Boltzmann equation in electrolyte solution theory. *Cond. Matt. Phys.* **2019**, *22*, 23801.

(53) Blum, L. *Theoretical Chemistry: Advances and Perspectives*; Academic: New York, 1980; Vol. 5; pp 1–66.

(54) Todorov, I. T.; Smith, W.; Trachenko, K.; Dove, M. T. DL_POLY_3: new dimensions in molecular dynamics simulations via massive parallelism. *J. Mater. Chem.* **2006**, *16*, 1911–1918.

(55) Weeks, J. D.; Chandler, D.; Andersen, H. C. Role of repulsive forces in determing the equilibrium structure of simple liquids. *J. Chem. Phys.* **1971**, *54*, 5237–5247.

(56) Andersen, H. C.; Weeks, J. D.; Chandler, D. Relationship between the hard sphere fluid and fluids with realistic repulsive forces. *Phys. Rev. A* **1971**, *4*, 1597–1607.

(57) Carnie, S.; Chan, D. Y. C.; Gunning, J. S. Electrical Double Layer Interaction between Dissimilar Spherical Colloidal Particles and between a Sphere and a Plate: The Linearized Poisson-Boltzmann Theory. *Langmuir* **1994**, *10*, 2993–3009.

(58) Morse, P. M.; Feshbach, H. *Methods of theoretical physics*; McGraw-Hill: New York, 1953.

(59) Stakgold, I. *Boundary value problems of mathematical physics*; Macmillan Co., New York, 1968.

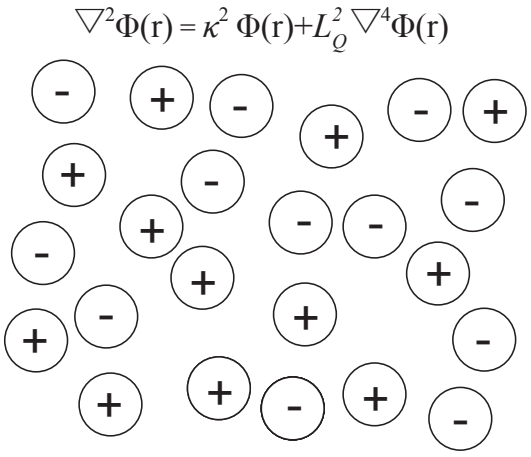

For Table of Contents Only